Rectifier Load Analysis for Electric Vehicle Wireless Charging System using Fuzzy Logic Controller

K Sathyesh, P. Ravikanth, D. Raveendhra
[1]M.Tech Scholar, Power Electronics Group, Gokaraju Rangaraju Institute of Engineering & Technology, Telangana, India
[2,3]Associate Professor, Gokaraju Rangaraju institute of engineering & technology, Telangana, India

ABSTRACT: This research looks at the rectifier load used in wireless charging systems for electric vehicles (EVs), as well as the implications for compensatory network design and system load prediction. To begin, create a rectifier load model that includes both resistance and inductance components to calculate its equivalent input impedance & may be estimated independently using the circuit characteristics of the rectifier. Then, Using the results of the planned rectifier load study, a compensation network model strategy is provided. A secondary side load estimating approach and a primary side load estimating approach, both of which rely only on observed voltages, have also been presented & consider the load on the rectifier in the case of system parameter fluctuations, the presented techniques demonstrate high accuracy and robustness. Scheduled fuzzy logic based on a controller that takes into account both the system voltage profile and the state of charge in the EV's battery. The goal of the fuzzy inference system is to prevent grid under voltage, flatten the system loading profile, and ensure that a given number of various EVs remain charged and connected fairly close to the system.

Keywords: Wireless charging system, rectifier load

I. INTRODUCTION

The advantages of an electric vehicle (EV) wireless charging system (WCS) are flexibility, comfort, space savings, and so on. As a result, it has garnered a great deal of attention. In recent years, both stationary & dynamic wireless EV charging systems have endure investigated & deployed in various demonstrations [1,2]. In EV WCS, a DC converter and output filter capacitor are utilized to convert AC which has high frequency to DC for charging the battery. To build the system or control strategy, in general, the DC converter and the circuit that follows it are equivalent to a pure resistance load [3,4]. A conventional way considering creating an analogous relationship between rectifier input impedance & rectifier output impedance near employ coefficient $8/\pi^2$ & system's load resistance [5]-[6]. However, at high frequencies, stray parameters & non-ideal device behavior's become visible [7]. In addition, the input inductance and other factors might have an effect on the rectifier's input impedance. As a result, if the WCS rectifier input impedance is treated as a pure resistance, it will cause some aberrations. In truth, The EV wireless charging platform's rectifier input impedance comprises both a resistance and an inductance component [7]-[9]. It preserves abide expressed in terms about a series about equivalent resistance & inductance values [9] - [10]. Even though there is no practical way for determining the equivalent load impedance of a Wireless Charging system's rectifier, a few previous research may be useful. The state space model may be used to explain the converter and its associated inductance and capacitance circuitry, considering stray resistances & forward voltage drop of diode [12] - [14]. This may be used to compute the equivalent load impedance of a wireless charging system's rectifier. Non-linear switching mechanisms and circuit simulations might potentially be used to look into the matter [15].

The non-linear behavior of converter load may complicate the architecture of its system compensation network. Compensation systems, however we all know, are critical to system functionality [16] and can be configured to provide max. efficiency, max. power, or conjugate matching [17]-[18]. rectifier load usually expressed like a pure resistance [19-21]. However, operating states of compensation network may be affected with operation modes of WCS rectifier load [22]. because of this, when constructing compensation network, actual equivalent input impedance about WCS rectifier load should be taken into account. WCS load estimation has had same issue. effects of rectifier load may complicate load estimating equations [23], resulting in increased computation & control complexity. because of this, most load estimate, detection, & optimal load tracking persists done using a pure resistance load [24-26]. Another scenario when voltages & currents. Both would commonly measure considering load estimate in order to compute primary side impedances [27]-[28]. Because phase delays about voltage & current sensors or probes differ at high frequencies, some discrepancies may be introduced into estimation process. Furthermore, estimation method's robustness critical. Its outcomes are studied via parameter derivation, root locus, Nyquist curve, bode graph, or directly computing outcomes under different parameter modifications.

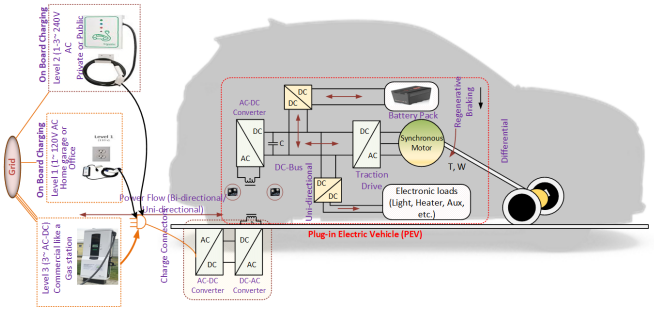

Fig.1: Principal diagram for Wireless charging system in electric vehicles

II. LITERATURE REVIEW

Wireless power transfer (WPT) a technology a certain has potential of freeing people annoying cables. In fact, WPT uses a basic principle known like inductive power transfer a certain has endure around considering at least 30 years (IPT). In recent years, WPT technology has advanced at a remarkable pace. transfer distance grows commencing a few millimeters to several hundred millimeters at kilowatt power levels among a grid-to-load efficiency about more than 90% WPT now very appealing considering usage in electric vehicle (EV) charging applications, including stationary & dynamic charging scenarios, thanks for these advancements. This chapter examines WPT technologies by considering EV wireless charging challenges about charging time, range, & cost Furthermore, among mass market adoption about EVs, battery technology no longer significant. It hoped a certain researchers resolve continue near push forward & further development about WPT, in addition, extension about EVs, inspired with the state-of-the-art achievements.

The Korea Advanced Institute about Science & Technology (KAIST), Daejeon, Korea, invented Online Electric Vehicle (OLEV), an innovative electric transportation system a certain remotely picks up electricity commencing power transmitters

buried below. Unlike a traditional electric car, which requires extensive downtime considering recharging, OLEV's battery may abide charged while vehicle in motion. TIME Magazine named OLEV like one about "50 Best Innovations about 2010," & it being examined like a possible option considering South Korea's next-generation electric public transit system. OLEV prototype has endure completed, & commercialization process already underway. One about most important aspects in ensuring system's successful commercialization determining how to redistribute power transmitters scheduled certain routes in a cost-effective manner, in addition, how to assess vehicle's battery capacity. no. of power transmitters & battery capacity have a direct impact scheduled initial infrastructure cost. In this study, we first discuss system design difficulties a certain arise when a mass transit system uses OLEVs. Next, we'll look at a near arrange economically power transmitters & determine battery capacity about OLEV-based mass transportation system, a mathematical model & an optimization method was used. solution method considering optimization problem particle swarm optimization (PSO) algorithm. near demonstrate correctness about mathematical model & sensitivity analysis, numerical issues among sensitivity analysis persist presented.

This research presents a method considering automatic "maximum energy efficiency tracking" (MEET) operating considering wireless power transfer systems. proposed technique follows highest energy efficiency operating points about a wireless power transfer system aside using switched mode converter in receiver module near imitate ideal load value aside locating operating point among lowest input power considering a given output power. concept does not require any wireless communication feedback because searching done scheduled transmitter side. Under both week & strong magnetic coupling circumstances, control strategy has endure effectively demonstrated in a 2-coil system. findings about experiments persist given near back up theory.

III. Rectifier Load Analysis and Calculation

In an EV wireless charging system, full-bridge diode ac to dc converter, most popular topology. DSLCC compensation networks preserve also provide various acceptable design degrees about freedom at same time near accomplish multiple system performance K_{pi}. Furthermore, it is possible to design it such that the whole resonant frequency is regardless of the load state [16,22]. As a result, we will examine rectifier load on the base of this type of architecture.

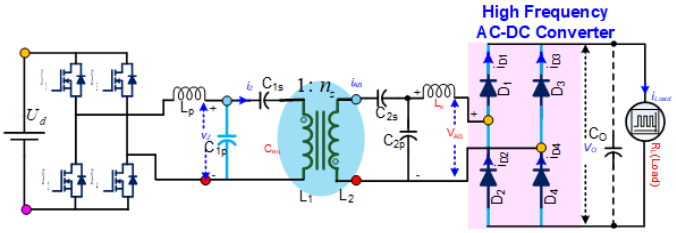

Fig.2. EV WCS with full-bridge diode converter & DS LCC compensation networks.

Figure 2 depicts an EV WCS comprised of a full-bridge dc converter and DS LCC compensation topology, wherein U_d is a DC voltage source, G_1-G_4 is a high frequency inverter, and D_1-D_4 is a full-bridge converter; The left side compensation network is made up of L_P, C_{1S}, and C_{1P}, whereas the right side compensation network is made up of L_s, C_{2S}, and C_{2P}.; L_1 and L_2 persist transmit & receive coils' self-inductances; M mutual inductance between them; C_{in} and C_o persist system input & output filter capacitors; & R_L, system load resistor. It should abide noted a certain in real world, WCS load an EV power battery, which acts like a voltage source series due near its parasitic resistance. power battery, scheduled other hand, may abide equal near a load resistance R_L [1,19], value about which may abide estimated aside dividing voltage scheduled power battery aside current flowing through it. Furthermore, rectifier circuit includes full-bridge rectifier, its input inductor, output filter capacitor, & load resistor. Despite fact a certain following study based scheduled a specific system, it is applicable for different converter and compensation configurations.

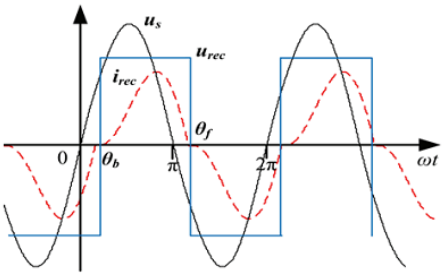

Fig. 3. Waveform diagrams for source voltage, rectifier input voltage & rectifier input current.

Because of the influence of DC converter input inductance, waveform about rectifier input current i_{rec} seems near abide distorted in Fig.3. like a result, i_{rec} fundamental wave lags behind u_{rec} fundamental wave. Because of this, rectifier input impedance contains not only a resistance element, but also an inductance element. Furthermore, considering all voltage & current waveforms, Fig.3 shows a certain positive & negative half-cycles persist symmetric. Due to this, we only need to think of the positive half-cycle, & negative half-cycle would be calculated using symmetry. analogous circuit about rectifier circuit in positive half cycle shown in Fig.4, taking into account stray characteristics & diode forward voltage drop where u_{dio} denotes forward voltage drop across diode; R_{dio} denotes resistance of diode conduction. R_{Ls}, & R_{co} are L_o & C_o stray resistances, respectively; load voltage & current could be represented with u_d & i_d, respectively..

Fig. 4. Equivalent circuit for bridge converter circuit in positive half cycle

I_{rec} specified like state variable x_1 in analogous circuit, while voltage scheduled C_o defined like state variable x_2. input variables u_s & u_{dio} persist used, while output variable u_d used. In positive half cycle, state space equation about rectifier circuit given with (1a).

$$\begin{bmatrix} x_1' & x_2' \end{bmatrix} = A\begin{bmatrix} x_1 & x_2 \end{bmatrix} + B\begin{bmatrix} u_s & u_{dio} \end{bmatrix}$$
$$y = C\begin{bmatrix} x_1 & x_2 \end{bmatrix} \quad (1)$$

Here, impedance matrixes A, B, and C are given by (1b).

$$A = \begin{bmatrix} \left(\frac{-1}{L_s}\right)\left(R_{Ls} + 2R_{dio} + \frac{R_{Co}R_L}{R_{Co}+R_L}\right) & \left(\frac{-1}{L_s}\right)\left(1 - \frac{R_{Co}}{R_{Co}+R_L}\right) \\ \frac{R_L}{C_o(R_{Co}+R_L)} & \end{bmatrix}$$

$$B = \left[\frac{1}{L_s} \ \frac{-2}{L_s} \ 0 \ 0\right], C = \left[\frac{R_{Co}R_L}{R_{Co}+R_L} \ 1 - \frac{R_{Co}}{R_{Co}+R_L}\right] \quad (1.b)$$

According to waveform diagrams in Fig.2, input variables & initial values about state variables can be given with (2); where, frequency of system angle; & forward voltage drop of diode represented like a constant value V_{dio}. Because there persist only a few R_{co} is relatively modest, their effects may be overlooked, & initial value about x_2 could be roughly similar near DC voltage variable, V_d. Furthermore, amplitude about u_s specified like V_s, & it influenced by WCS characteristics like source voltage, mutual inductance, & so on. However, u_{rec} & i_{rec} amplitudes are proportional to V_s. because of this, V_s may be considered as a known variable.

$$u_{s+} = V_s \sin sin(\omega t + \theta_b), u_{dio} = V_{dio}, x_+(0) = \left[0, V_d\right]^T \quad (2)$$

Value of V_{dio} & voltage drops scheduled R_{dio} & R_{ls} are substantially smaller than ones scheduled V_s & V_d in regular WCS working conditions. due to this, voltage scheduled L_s about comparable to $V_s \sin\theta - V_d$, according to relationship between voltage scheduled an inductor & current flowing through it, (3)could be used to denote i_{rec}.

$$i_{rec} = \frac{1}{\omega L_s}\int_{\theta_b}^{\theta}(V_s \sin sin\,\theta - V_d)d\theta \quad (3)$$

As seen in Fig.2, $i_{rec}=0$, when $\theta=\theta_f=\theta_b+\pi$. So, one relationship between and θ_b may be obtained & provided with (4).

$$V_d = \frac{2V_s}{\pi}\cos cos\,\theta_b \quad (4)$$

(5) may also be used to compute the DC load current I_d. This is the positive half cycle's average i_d value

$$I_d = \frac{1}{\omega\pi L_s}\int_{\theta_b}^{\theta_b+\pi}\int_{\theta_b}^{\theta}(V_s \sin sin\,\theta - V_d)d\theta$$

$$I_d = \frac{1}{\omega\pi L_s}\left[V_s(2\sin sin\,\theta_b + \pi\cos cos\,\theta_b) - V_d\frac{\pi^2}{2}\right] \quad (5)$$

Because $I_d = V_d/R_L$, another relationship between V_d and θ_b may be obtained & provided with(6).

$$V_d = \frac{V_s\left(2\sin sin\,\theta_b + \pi\cos cos\,\theta_b\right)}{\pi\left(\frac{\omega L_s}{R_L}+\frac{\pi}{2}\right)} \quad (6)$$

They shall derived commencing (4) & (5) based scheduled two relationships between V_d & θ_b (6). (7) gives expression about θ_b, & their relationships may also be used for getting expression for V_d. According to Equation (7), phase difference between us & u_{rec} (or I_{rec}) mostly determined with L_S & R_L, & relatively unaffected aside other WCS factors. We may claim a certain other elements about WCS have little effect scheduled rectifier circuit because the u_{rec} and i_{rec} amplitudes persist basically proportional to one about u_s like indicated earlier, & rectifier load may be separated near examine its equivalent input impedance. It should be noted that, according to, rectifier circuit appears to be equivalent to a pure resistance R_L. This comparable relationship, however, preserve only be used considering (7) when computing phase angle b, & not considering any other element about rectifier load analysis.

$$\left(\frac{\omega L_s}{R_L}\right) \quad (7)$$

After obtaining V_d & θ_b, eqn.(8) may be used for calculating full response about rectifier circuit in positive half cycle; where $\emptyset(t)$ rectifier circuit's characteristic matrix; the component before the addition sign would be used to resolve the zero-input response, while the other component is utilized towards the end to get the zero-state response. According to (8), time domain expressions about u_{rec} & i_{rec} can be calculated.

$$x(t) = \emptyset(t)x(0) + \int_0^t \emptyset(\tau)Bu(t-\tau)d\tau \quad (8)$$

Finally, using Fourier transform, fundamental wave amplitudes & phase angles about u_{rec} & i_{rec} may abide computed & expressed as U_{rec_fd}, I_{rec_fd}, φ_{urec_fd} & φ_{irec_fd}. as a result, equivalent input impedance about a WCS rectifier load (9), where R_e & L_e persist rectifier load's series equivalent resistance & inductance. Because harmonics' power substantially lower than fundamental waves, only fundamental wave examined, and would be determined using Fourier transform. Furthermore, mathematical procedure suggests a certain parameter about rectifier circuit resolve affect R_e & L_e as a result, method's robustness near parameter fluctuation must abide investigated. However, because robustness related near some complex or non-linear operations, theoretical approaches like calculating derivative & root locus cannot provide a simple & obvious way to examine robustness in this scenario. as a result, based scheduled actual parameter values, this issue will be resolved by examining the Section V.

$$R_e = \left(\frac{U_{rec\_fd}}{I_{rec\_fd}}\right)\cos cos\left(\varphi_{urec_{fd}} - \varphi_{irec_{fd}}\right),$$

$$L_e = \left(\frac{U_{rec\_fd}}{I_{rec\_fd}}\right)\frac{\sin sin\left(\varphi_{urec_{\_fd}} - \varphi_{irec_{\_fd}}\right)}{\omega} \quad (9)$$

To summarize, preceding analysis indicates a certain equivalent impedance about rectifier load has both resistance & inductance components. Furthermore, series equivalent resistance & inductance may abide estimated independently using rectifier circuit specifications, & results persist mostly unaffected aside other WCS characteristics. As a result, rectifier load may be separated from other WCS components.

IV. DESIGNING OF COMPENSATION NETWORK

Because the DC converter load has been separated from other sections of the WCS, we will present a compensation circuit design approach depending on the rectifier load analysis and previous studies [16-18]. Furthermore, the suggested technique will isolate the primary and secondary side designs even further, making the WCS compensation network design easier. DS LCC compensation networks persist used here, just like they persist in rectifier load analysis. As noted above, input inductance of rectifier, L_s should be large enough near keep it in CCM condition, therefore we'll double-check it before designing compensation network. primary side compensation inductance also important L_p assumed as known, thus design procedure in this part simply uses four compensation capacitors.

Fig.5. Equivalent circuit for the secondary side which considers impedance equivalent to rectifier load.

The secondary side first examined, & equivalent circuit given in Fig.4; where series equivalent resistance, R_e & equivalent inductance, L_e may be used for indicating rectifier load, & R_2, receiving coil resistance. Z_{s1} defined as impedance, following secondary side series compensation capacitor, C_{2s}, it is shown in Fig.4, & its expression (10);

$$re\left(Z_{s1}\right)=\frac{\frac{R_e^{'}}{\left(\omega C_{2p}\right)^2}}{\left(\frac{1}{\omega C_{2p}}-\omega L_e^{'}\right)^2+\left(R_e^{'}\right)^2}$$

$$im\left(Z_{s1}\right)=\frac{\frac{L_e^{'}}{\omega\left(C_{2p}\right)^2}\left(\frac{1}{\omega C_{2p}}-\omega L_e^{'}\right)-\frac{\left(R_e^{'}\right)^2}{\omega C_{2p}}}{\left(\frac{1}{\omega C_{2p}}-\omega L_e^{'}\right)^2+\left(R_e^{'}\right)^2} \quad (10)$$

As a result, the equation for the efficiency η_c may be computed and provided by (11); wherein η_c is the efficiency of inverter output over rectifier load impedance; R1 is the transmit coil resistance; X_{se}=im(Z_{s1})+ ωL_2-1/(ωC_{2s}).

$$\eta_c=\frac{re\left(Z_{s1}\right)\omega^2M^2}{\left(re\left(Z_{s1}\right)+R_2\right)\omega^2M^2+\left(re\left(Z_{s1}\right)+R_2\right)^2R_1+R_1X_e^{\ 2}} \quad (11)$$

Equation (11) shows a certain in order near achieve optimal efficiency, two requirements must abide met. first X_{se} =0, which reduces denominator η_c.The other a certain receive coil's load resistance equal near ideal load resistance. R_{opt}, like instructed aside (12);

$$re\left(Z_{s1}\right)=R_{opt}=\sqrt{R_2^2+\omega^2M^2\frac{R_2}{R_1}} \quad (12)$$

The secondary side parallel compensating capacitor, C_{2p} may be computed & given by using (10) & (12). (13). secondary side series compensation capacitor, C_2 may likewise abide solved using value about C_{2p} & equation X_{se} =0. According near preceding study, secondary side compensating capacitors may be constructed separately from primary side ones, & their primary goal is to maximize system efficiency.

$$C_{2p}=\frac{\omega L_e^{'}+\sqrt{\omega^2L_e^{'2}-\left(\omega^2L_e^{'2}+R_e^{'2}\right)\left(1-\frac{R_e^{'}}{R_{opt}}\right)}}{\omega\left(\omega^2L_e^{'2}+R_e^{'2}\right)} \quad (13)$$

The primary side then investigated, & equivalent circuit given in Fig.5; where u_{inv} denotes inverter output equivalent voltage source; RLP denotes stray resistances about L_P; & R_{es} denotes equivalent resistance about secondary side, where C_{2s} and C2p may appropriately be designed, & R_{es}= ω^2M^2 /(R_{opt}+R_2) .

Fig. 6. Equivalent circuit for primary side, for a well-designed secondary side

$$re\left(Z_{p1}\right)=\frac{\left(\frac{R_{es}+R_1}{\omega^2C_{1p}^{\ 2}}\right)}{\left(\frac{1}{\omega C_{1p}}-\omega L_1+\frac{1}{\omega C_{1s}}\right)^2+\left(R_{es}+R_1\right)^2}$$

$$im\left(Z_{p1}\right)=\frac{\left(\omega L_1-\frac{1}{\omega C_{1s}}\right)X_{pe}-\left(R_{es}+R_1\right)^2}{\omega C_{1p}\left(X_{pe}^{\ 2}+\left(R_{es}+R_1\right)^2\right)} \quad (14)$$

As shown in Fig.5, Z_{p1} i is mentioned as impedance after primary side compensation inductor, L_p, & its expression given aside (14); where, X_{pe}=ω_{l1}-1/(ωC_{1s})-1/(ωC_{1p}); $r_e(Z_{p1})$ means real part about Z_{p1}; im(Z_{p1}) imaginary part about Z_{p1}. primary side has two compensation capacitors among two degrees of freedom considering in design, similar like secondary side. due to this, two design targets might abide added to this list. Making WCS output rated power first step. (15) where U_{inv} denotes RMS value about u_{inv}, P_{or} denotes rated WCS output power, & η_r denotes rated WCS efficiency.

$$\frac{U_{inv}^2}{re\left(Z_{p1}\right)}=\frac{P_{or}}{\eta_r} \quad (15)$$

The second design goal is to maintain a particular inductance in primary side compensation network's input impedance in order to achieve smooth switching in inverter. where L_{soft} denotes inductance required considering soft switching in inverters.

$$\frac{im\left(Z_{p1}\right)}{\omega}+L_p=L_{soft} \quad (16)$$

Values about main side compensation capacitors, C_{1s} and C_{1p} can be determined by simultaneously solving (15) & (16), which could be unaffected by secondary side design procedure. It's also worth noting a certain these equations don't always have an analytical solution. This circumstance necessitates employment about numerical solution methods.

Finally, considering design purposes, primary & secondary side compensation networks have endure disconnected. In addition, four compensating capacitors among four degrees of freedom persist constructed aside taking into account four system performance indicators, including maximizing efficiency & minimizing load resistance, Increasing WCS output rated power & achieving gentle inverter switching Furthermore, for achieving better outcomes, computed values of planned compensation capacitors must be fine-tuned in practice.

V. LOAD ESTIMATION METHODS

The results about rectifier load study may be utilised to estimate system load in WCS, which uses high frequency signals. traditional load assessment methods persist mainly based on a pure resistance load & require both high frequency voltage & current [24,27]. At high frequencies, phase delays of voltage & current sensors or probes may differ, Oscilloscopes & power analyzers, considering example, use them. These various phase delays preserve cause some phase angle discrepancies between measured voltage & current, which resolve influence accuracy about impedance calculation, especially when phase angle close to 90 degrees.

We present a load estimation method based on secondary side high frequency voltages for tackling this problem. for acquiring positive zero crossing times, positive zero crossings about rectifier input voltage (u_{rec}) & voltage before rectifier input inductor (the voltage scheduled C_{2p} considering LCC topology) are first detected. Then, use terms t_{ucs} & t_{urs} to represent positive zero crossing time about voltage before rectifier input inductor & subsequent positive zero crossing time of rectifier input voltage, respectively. According near relationship shown in, load estimation expression (17). Finally, since

$$R_{L_{Sesti}}=\frac{\omega L_s}{tan(\omega(t_{urs}-t_{ucs})} \quad (17)$$

The WCS rectifier load was taken into account when developing suggested secondary side load calculation method. In addition, this approach uses just high frequency voltages & does not need any current. Due to this,

discrepancies caused aside varying phase delays between measured voltage & current would be avoided. Furthermore, proposed approach limited to detecting positive zero crossing timings, However, voltage amplitudes & RMS values may not be required. corresponding measurements & computations can be simplified as a result.

In most cases, however, measured signals must be transferred to primary side via wireless communication considering system optimization or control. We also proposed a load estimating method based scheduled primary side high frequency voltages to overcome issues caused with wireless communication. voltage following inverter output inductor (the voltage on C_{1p} of LCC topology) & inverter output voltage (u_{inv}) are used here.

VI. Fuzzy Logic Controller

Fuzzy logic used successfully in a variety about control applications. Almost every item purchased has some form about fuzzy control. Controlling room temperature using a forced air system, anti-lock brakes in vehicles, traffic signal control, clothes washers, massive financial frameworks, & so scheduled are just a few examples. A control gadget a collection about real-world components are used to alter behavior about another physical framework so it exhibits desired characteristics. following are some arguments about why fuzzy logic used in charge frameworks.

- When utilizing regular control, it is critical to completely understand the model and the objective justification. This makes it tough to implement in some situations.
- We can create a regulator utilizing human knowledge and expertise by employing fluffy logic for control
- The fuzzy control rules, or IF-THEN standards, are great for creating a control framework. The key sections of the FLC are mentioned below–

Fuzzifier − The fuzzifier's role would be to convert fresh information values into fluffy ones.

Fuzzy Knowledge data stored in base, & almost all about data yield fluffy connections. It also has an enrollment feature a certain shows information factors considering fluffy principal foundation & yield factors considering plant balanced out.

Fuzzy Rule Base It maintains record of every spatial interaction's movement.

Derivation Engine It preserve abide used like a part in any FLC. Essentially, it does rudimentary reasoning in order near display human choices.

DE fuzzifier − The objective of the DE fuzzifier is to transform the fluffy characteristics acquired from the fluffy deduction motor into new qualities.

Fig.7 Membership functions for error.

Fig.8 Membership function for Differentiated-error.

VII. Simulation results

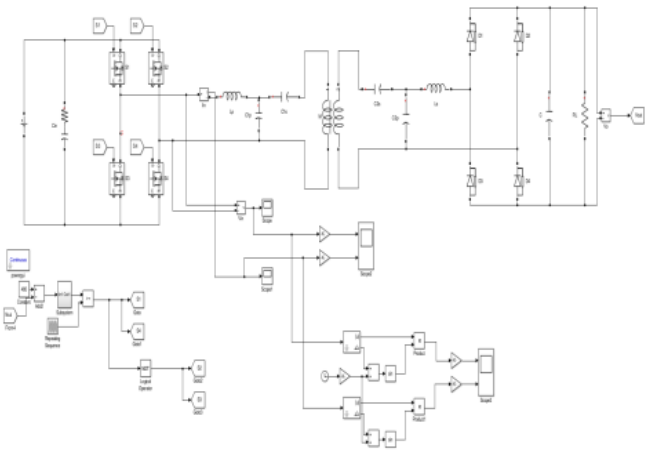

Fig 9. Simulink model of proposed system

Fig10. fuzzy system model

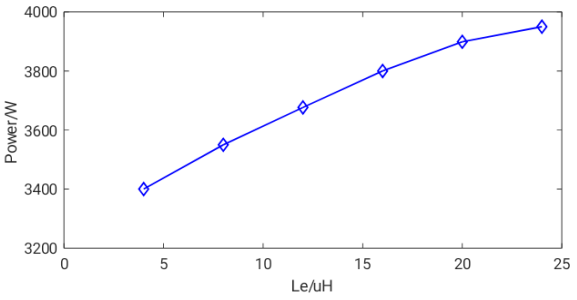

(a)

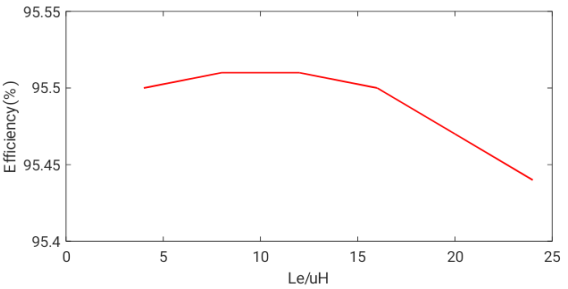

(b)

FIG.11 (a) Simulation results about L_e effects scheduled output power. (b) Simulation results for Le effects efficiency

According to Fig.11.a & Fig.11.b, the effect of L_e on efficiency is negligible. When L_e fluctuates, the output power changes from around 3.4 kW to more than 3.9 kW. In light of the ratings. The system output power is 3.3 kW, and the change range is greater than 15% under the effect of the equivalent inductance. As a result, if the compensation circuits are constructed without taking L_e into account, the output power will be considerably affected, and the overall output power will deviate greatly from the rated one.

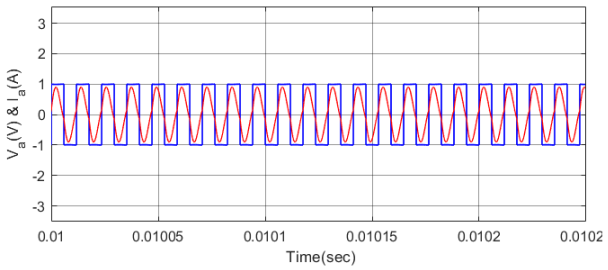

Fig12.a Waveform of (a) Rectifier input voltage and (b) input current

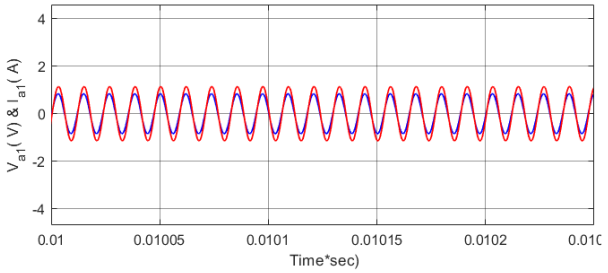

Fig.12.c calculated fundamental waves.

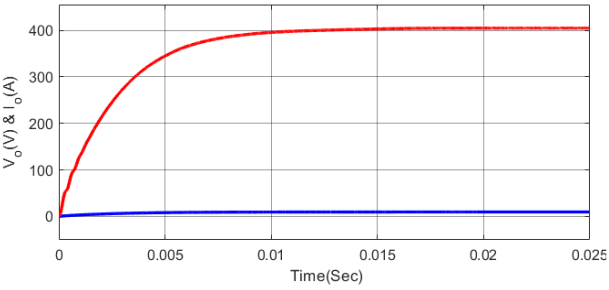

FIG.12.d converter output voltage and current

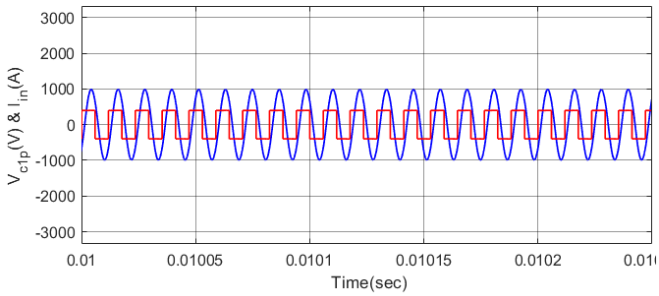

Fig.13.a Measured voltages used considering primary side load estimation

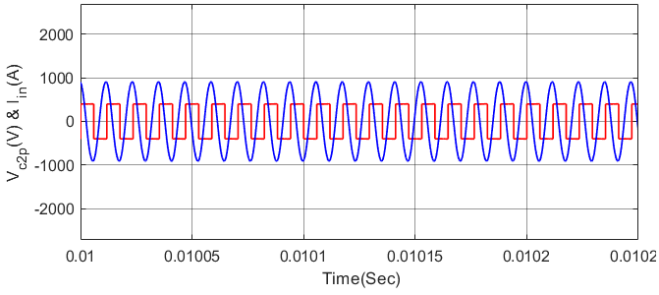

Fig.13.b Measured voltages used considering secondary side load estimation

Fig.12.a & Fig.12.b are the rectifier input voltage and current respectively through which the fundamental waves are computed by performing FFT (Fast Fourier Transform) which are shown in the Fig.12. c. The measured voltages in Fig. 13.b are used to estimate secondary side loads, whereas those in Fig. 13a are used to estimate primary side loads. The positive zero crossing timings may be easily derived from the observed data using these research findings and It is possible to evaluate the system load resistance.

VIII. Comparison of PI and Fuzzy Logic Controller

In this WCS of EV, a PI controller was used for avoiding the voltage variations caused with different spacing between two coils, resulting in a constant voltage & constant current near load. Simulations & comparisons among a single PI controller were used for verifying efficiency of this control system. A fuzzy logic controller was also developed, which proved more reliable than PI controller because output voltage did not undershoot.

In future study, the neuro-fuzzy controller should be designed in such a manner that perhaps the input and output information for training fully duplicates the characteristics of the learnt FIS data.

IX. CONCLUSION

This study investigates the rectifier load used in an EV WCS in depth. Depending on the schedule produced EV WCS the suggested rectifier load calculation technique, compensation circuit design approach, and secondary and main side load estimation techniques have all been verified. Despite the fact that this publication's study focused on a specific system, they continue to be utilized in a number of applications, such as WCS that employ various rectifier or compensation network topologies, and so on. They'll be useful in terms of system design and control in order to ensure that EV wireless charging systems are reliable and efficiency. Scheduled fuzzy controllers, on the other hand (which are non-linear controllers), are capable of correctly handling these impacts and non-linearities in systems, hence improving system performance and decreasing development time and costs.

X. REFERENCES

[1]. S. R. Khutwad and S. Gaur, "Wireless charging system for electric vehicle," 2016 International Conference on Signal Processing, Communication, Power and Embedded System (SCOPES), 2016, pp. 441-445.

[2]. Y. J. Jang, Y. D. Ko and S. Jeong, "Optimal design of the wireless charging electric vehicle," 2012 IEEE International Electric Vehicle Conference, 2012, pp. 1-5.

[3]. X. Hu, Y. Wang, Y. Jiang, W. Lei and X. Dong, "Maximum Efficiency Tracking for Dynamic Wireless Power Transfer System Using LCC Compensation Topology," 2018 IEEE Energy Conversion Congress and Exposition (ECCE), 2018, pp. 1992-1996.

[4]. D. Ahn, S. Kim, J. Moon and I. Cho, "Wireless Power Transfer with Automatic Feedback Control of Load Resistance Transformation," in IEEE Transactions on Power Electronics, vol. 31, no. 11, pp. 7876-7886, Nov. 2016.

[5]. Kline, Mitchell & Izyumin, Igor & Boser, Bernhard & Sanders, Seth. (2011). Capacitive power transfer for contactless charging. 1398 - 1404. 10.1109/APEC.2011.5744775.

[6]. Thayalan, Daniel & Park, Joung-Hu. (2015). Wide Air-Gap Transformer Model for the Design-Oriented Analysis of Contactless Power Converters. IEEE Transactions on Industrial Electronics. 62. 1-1. 10.1109/TIE.2015.2423662.

[7]. M. Fu, Z. Tang and C. Ma, "Analysis and Optimized Design of Compensation Capacitors for a Megahertz WPT System Using Full-Bridge Rectifier," in IEEE Transactions on Industrial Informatics, vol. 15, no. 1, pp. 95-104, Jan. 2019.

[8]. A. Berger, M. Agostinelli, S. Vesti, J. Á. Oliver, J. A. Cobos and M. Huemer, "Phase-shift and amplitude control for an active rectifier to maximize the efficiency and extracted power of a Wireless Power Transfer system," 2015 IEEE Applied Power Electronics Conference and Exposition (APEC), 2015, pp. 1620-1624.

[9]. E. Asa, K. Colak, M. Bojarski and D. Czarkowski, "A novel phase control of semi bridgeless active rectifier for wireless power transfer applications," 2015 IEEE Applied Power Electronics Conference and Exposition (APEC), 2015, pp. 3225-3231.

[10]. Y. Akihara, T. Hirose, S. Masuda, N. Kuroki, M. Numa and M. Hashimoto, "Analytical study of rectifier circuit for wireless power transfer systems," 2016 International Symposium on Antennas and Propagation (ISAP), 2016, pp. 338-339.

[11]. H. Li, J. Li, L. Huang, K. Wang and X. Yang, "A novel dynamic modeling method for wireless power transfer systems," 2015 IEEE Applied Power Electronics Conference and Exposition (APEC), 2015, pp. 2740-2743.

[12]. Y. Hara, T. Ohsato and H. Sekiya, "Pre- and Post-Regulation Control of High-frequency Magnetic-Resonance Wireless Power Transfer System with Class-D Rectifier," 2018 IEEE International Telecommunications Energy Conference (INTELEC), 2018, pp. 1-6.

[13]. Y. Guo, Y. Zhang, Q. Bo, Z. Liu, J. Meng and L. Wang,

"Approximate Linearization of Rectifier Load in Wireless Power Transfer Systems," 2020 IEEE PELS Workshop on Emerging Technologies: Wireless Power Transfer (WoW), 2020, pp. 74-78.
[14]. C. K. Lee, S. Kiratipongvoot, & S. C. Tan, “High-frequency-fed unity power-factor AC-DC power converter among one switching per cycle,” IEEE Trans. Power Electron., vol. 30, no. 4, pp. 2148-2156, April 2015.
[15]. Z. Bing, K. J. Karimi and J. Sun, "Input Impedance Modeling and Analysis of Line-Commutated Rectifiers," in IEEE Transactions on Power Electronics, vol. 24, no. 10, pp. 2338-2346, Oct. 2009.
[16]. Y. Chen, H. Zhang, C. -S. Shin, C. -H. Jo, S. -J. Park and D. -H. Kim, "An Efficiency Optimization-Based Asymmetric Tuning Method of Double-Sided LCC Compensated WPT System for Electric Vehicles," in IEEE Transactions on Power Electronics, vol. 35, no. 11, pp. 11475-11487, Nov. 2020.
[17]. M. Dionigi, M. Mongiardo and S. Koziel, "Surrogate-based optimization of efficient resonant wireless power transfer links using conjugate image impedances," 2014 44th European Microwave Conference, 2014, pp. 429-432.
[18]. F. Mastri, M. Mongiardo, G. Monti, L. Corchia, A. Costanzo and L. Tarricone, "Load-Independent Inductive Resonant WPT Links," 2019 IEEE International Conference on RFID Technology and Applications (RFID-TA), 2019, pp. 11-15.
[19]. Q. W. Zhu, L. F. Wang, & C.L. Liao, “Compensate capacitor optimization considering kilowattlevel magnetically resonant wireless charging system,” IEEE Trans. Ind. Electron., vol. 61, no. 12, pp. 6758-6768, Dec. 2014.
[20]. Y. Zhaksylyk and M. Azadmehr, "Comparative Analysis of Inductive and Capacitive Feeding of Magnetic Resonance Wireless Power Transfer," 2018 IEEE PELS Workshop on Emerging Technologies: Wireless Power Transfer (Wow), 2018, pp. 1-5.
[21]. S. Jeong, T. Lin and M. M. Tentzeris, "Range-adaptive Impedance Matching of Wireless Power Transfer System Using a Machine Learning Strategy Based on Neural Networks," 2019 IEEE MTT-S International Microwave Symposium (IMS), 2019, pp. 1423-1425.
[22]. T. Kan, F. Lu, T. Nguyen, P. P. Mercier and C. C. Mi, "Integrated Coil Design for EV Wireless Charging Systems Using LCC Compensation Topology," in IEEE Transactions on Power Electronics, vol. 33, no. 11, pp. 9231-9241, Nov. 2018.
[23]. J. P. W. Chow, H. S. H. Chung and C. S. Cheng, "Online regulation of receiver-side power and estimation of mutual inductance in wireless inductive link based on transmitter-side electrical information," 2016 IEEE Applied Power Electronics Conference and Exposition (APEC), 2016, pp. 1795-1801.
[24]. J. Yin, D. Lin, C. K. Lee and S. Y. R. Hui, "Load monitoring and output power control of a wireless power transfer system without any wireless communication feedback," 2013 IEEE Energy Conversion Congress and Exposition, 2013, pp. 4934-4939.
[25]. J. Lu, G. Zhu, H. Wang, F. Lu, J. Jiang and C. C. Mi, "Sensitivity Analysis of Inductive Power Transfer Systems with Voltage-Fed Compensation Topologies," in IEEE Transactions on Vehicular Technology, vol. 68, no. 5, pp. 4502-4513, May 2019.
[26]. T. Zhang, M. Fu, C. Ma and X. Zhu, "Optimal load analysis for a two-receiver wireless power transfer system," 2014 IEEE Wireless Power Transfer Conference, 2014, pp. 84-87.
[27]. E. Chung, G. C. Lim, J. Ha and K. Y. Kim, "Output voltage control for series-series compensated wireless power transfer system without direct feedback from measurement or communication," 2017 IEEE Energy Conversion Congress and Exposition (ECCE), 2017, pp. 4035-4040.
[28]. S. Mukherjee et al., "Control of Output Power in Primary Side LCC and Secondary Series Tuned Wireless Power Transfer System without Secondary Side Sensors," 2020 IEEE Energy Conversion Congress and Exposition (ECCE), 2020, pp. 5532-5536.